Available online at www.sciencedirect.com
ScienceDirect
Applied Catalysis B: Environmental 80 (2008) 122–128
APPLIED CATALYSIS B: ENVIRONMENTAL
www.elsevier.com/locate/apcatb

Electrocatalytic hydrodehalogenation of pentachlorophenol at palladized multiwalled carbon nanotubes electrode

Chunyue Cui [a,b], Xie Quan [a,b,*], Hongtao Yu [a,b], Yanhe Han [a,b]

[a] School of Environmental and Biological Science & Technology, Dalian University of Technology, Dalian 116024, China
[b] Key Laboratory of Industrial Ecology and Environmental Engineering, Ministry of Education, China

Received 28 June 2006; received in revised form 20 November 2007; accepted 22 November 2007
Available online 3 January 2008

Abstract

The palladized multiwalled carbon nanotubes (MWCNTs) electrode was prepared for electrocatalytic hydrodehalogenation (HDH) of pentachlorophenol (PCP). The MWCNTs grew directly on graphite by chemical vapor deposition (CVD), and Pd was loaded on MWCNTs with electrochemical deposition. The MWCNTs and Pd catalyst were characterized by scanning electron microscopy (SEM), transmission electron microscopy (TEM), nitrogen adsorption (BET surface area) and X-ray diffraction (XRD). The diameter and surface area of MWCNTs were 40–60 nm and 54 m^2/g, respectively. The particle size of Pd was about 13 nm. Electrocatalytic HDH of PCP by Pd/MWCNTs/graphite electrode was performed in H_2SO_4 anolyte separated by Nafion membrane H-cell. The complete degradation of 0.15 mM PCP was achieved at 180 min with the dechlorination efficiency being 96%, and the yield of cyclohexanone was 60% (7.4% current efficiency). Compared with the Pd/graphite electrode, the Pd/MWCNTs/graphite electrode exhibited higher dechlorination efficiency and hydrogenation activity of the carbon–carbon double bond for PCP. The effects of anolyte and potential on HDH, electrode stability were also investigated.

Keywords: Carbon nanotubes; Electrocatalytic hydrodehalogenation; Pentachlophenol; Palladium

1. Introduction

Halogenated phenol, a major group of pollutants used extensively as wood preservatives, pesticides, and as intermediates in the manufacture of pesticides, are causing great environmental concern [1]. These compounds are strongly resistant to chemical, physical or biological degradation [2]. The toxicity of these compounds is related with the halogen content, and increase with increasing number of halogen atoms [3]. Therefore, it is highly desirable to develop efficient and safe technology for the dehalogenation of halogenated organic compounds.

Hydrodehalogenation (HDH) was considered as a low-waste technology for detoxifying organic halogenated waste and regeneration of the initial raw materials [4]. Using molecular hydrogen as hydrogen donors, catalytic HDH of organic halogenated compounds was accepted as a practical choice, which was capable of carrying out in gas or liquid phase [5]. As there are harsh conditions in catalytic HDH, e.g., high temperature, or high pressure there are requirements for thermal, mechanical, and chemical stability of catalytic reactor components [6–9]. More severely, catalytic HDH often takes place at a gradually decreasing rate due to progressive poisoning or loss of the catalyst in some cases [10,11].

Recently, environmental electrochemical HDH of halogenated organic compounds has been suggested as a promising method for detoxification of halogenated wastes, which can successfully remove halogen atoms under mild experimental conditions at electrode loaded noble metal [12–15]. According to the literature [16], the mechanism of the electrocatalytic hydrogenolysis (ECH) of a carbon–halogen bond involves the steps described in Eqs. (1–4), where M, $(H)_{ads}M$ and $(R\text{-}X)_{ads}M$ represent electrode surface, chemisorbed hydrogen and the adsorbed organic substrate, respectively.

$$2H_2O + 2e^- + M \rightarrow 2(H)_{ads}M + 2OH^- \quad (1)$$

$$R - X + M \rightleftharpoons (R - X)_{ads}M \quad (2)$$

* Corresponding author. Tel.: +86 411 84706140; fax: +86 411 84706263.
E-mail address: quanxie@dlut.edu.cn (X. Quan).

0926-3373/$ – see front matter © 2007 Elsevier B.V. All rights reserved.
doi:10.1016/j.apcatb.2007.11.019

$$(R - X)_{ads}M + 2(H)_{ads}M \rightarrow (R - H_{ads}M + HX) \quad (3)$$

$$(R - H)_{ads}M \rightleftharpoons R - H + M \quad (4)$$

$$(H)_{ads}M + H_2O + e^- \rightarrow H_2 + OH^- + M \quad (5)$$

$$(H)_{ads}M + (H)_{ads}M \rightleftharpoons H_2 + M \quad (6)$$

The first step stands for the electroreduction of water (or hydrogen ions) with the formation of adsorbed hydrogen on the electrode surface (Eq. (1)). Then the adsorbed hydrogen reacts with the adsorbed substrate $(R - X)_{ads}M$ (Eq. (3)). There is a competition between hydrogenation (Eq. (3)) and desorption of hydrogen by an electrochemical (Eq. (5)) or chemical (Eq. (6)) pathway. This competition depends on a number of factors such as the substrate, electrode and reaction conditions [17].

Since their discovery at the beginning of the last decade [18], carbon nanotubes and nanofibers have received an increasing interest both from a fundamental point of view and for potential industrial applications [19–21]. The carbon nanotubes and nanofibers, which possess many special properties such as good electrical conductivity, high specific surface area, uniform pores, high H_2 uptake capacity [22] and good mechanical strength [23], have received increasing attention in recent years for their application as electrodic materials [24,25] or catalyst supports for hydrogenation reactions [26–28]. Those properties, which probably benefit to the reactions of Eqs. (1 and 2), exhibit potential applications of carbon nanotubes as novel materials for the catalyst carrier for some hydrogenation reactions electrode. Some researchers reported that the metal catalysts supported on multi-walled carbon nanotubes (MWCNTs) or carbon nanofiber exhibited much better activity than other carbon-based supports for some liquid phase catalytic hydrogenation reactions [26,27] and gas phase catalytic HDH [28]. But to the knowledge of authors, there has been no published study on the catalytic HDH taking MWCNTs as electrode.

In the present study, MWCNTs grew directly on graphite by chemical vapor deposition (CVD). Compared with the Pd/graphite electrode, this Pd/MWCNTs/graphite electrode is expected to provide enhanced surface catalytic properties for the HDH of PCP at low concentrations in aqueous solution.

2. Materials and methods

2.1. MWCNTs/graphite electrode preparation and modification

The MWCNTs grew directly on graphite sheet (20 mm × 30 mm × 2 mm) by chemical vapor deposition in a tube furnace [29]. MWCNTs were prepared by the catalytic decomposition of ferrocene-xylene mixture (Fe/C = 0.45%) with a feed rate of 0.08 mL/min at 900 °C and a gas mixture of Ar and H_2 (9:1) with a rate of 1000 mL/min at a pressure of 0.1 MPa for 2 h. After the reaction, the furnace was cooled to 450 °C under ambient Ar, and then to room temperature in flowing air.

The MWCNTs/graphite electrode was purified in 50% HNO_3 aqueous solution at 100 °C for 2 h. Surface oxidation of the MWCNTs was performed in a 4.0 M HNO_3−2.0 M H_2SO_4 (1:1) mixture at 100 °C for 5 h, and then the MWCNTs were washed with water and dried in vacuum for 8 h.

The morphology of MWCNTs was observed using scanning electron microscope (SEM, JSM-5600L, UK) and transmission electron microcopy (TEM, EM 400T, Phillips). The microscope assisted with energy dispersive X-ray (EDX) was used to analyze the approximate atomic composition on the examined surface.

The surface functional groups of modified MWCNTs were measured using Fourier transform spectrophotometer (FT-IR, Prestige-21, Shimadzu, Japan).

2.2. Electrodeposition of Pd

Palladized graphite and MWCNTs/graphite electrode were prepared by exposing graphite or MWCNTs/graphite to 40 mL solution of 2 mM $PdCl_2$ in 0.05 M H_2SO_4 for 6 h, and then deposited with a constant current of −5 mA for 4 h. The palladized electrodes were cleaned with water and then dried at 100 °C.

The electrodes were characterized by SEM and X-ray diffractometer (XRD, LabxXRD-6000, Shimadzu, Japan) with Cu Kα as radiation. Contents of Pd were determined by a flame atomic absorption spectrometer (AAS, Aanalyst 700, PerkinElmer, USA) from the diluted extract of aqua regia.

2.3. Electrochemical HDH

The electrolysis was carried out in a teflon-made H-cell (volume of electrolyte in each compartment was 60 mL) and the two compartments were separated by cation-exchange membrane (Nafion N324, Dupont Company, USA). The working electrode was a Pd/MWCNTs/graphite (20 mm × 30 mm × 2 mm), which was fixed with a nickel strip for electrical contact. The counter-electrode was a platinum foil with the dimension of 10 mm × 10 mm × 0.2 mm, and saturated calomel electrode (SCE) was used as the reference. The electrolysis was performed at a constant potential and 40 °C. The potential was controlled by a potentiostat from Shanghai Rex Instrument Co., China (Model DJS-292).

2.4. Analytical method

After electrolysis, the Pd/MWCNTs/graphite electrode was thoroughly rinsed with 1 M NaOH and ethanol. The solvent were combined with catholyte and the solution was filtered, saturated with NaCl, acidified to pH 1 and extracted with ethylacetate. The resulted sample was analyzed by GC/FID (GC-14C, Shimadzu, Japan) and HPLC (PU-1580, UV-1575, Jasco, Japan). The HPLC analysis was carried out at room temperature at a detector wavelength of 270 nm for phenol and 254 nm for PCP with a Kromasil ODS column (250 mm × 4.6 mm × 5 μm). The mobile phase was methanol: water (1% acetic acid) = 4:1 (v:v) at a flow rate of 1 mL/min.

Identification of intermediates was carried out using an HP 6890 GC coupled with 5973N mass selective detector (MSD) with a capillary column (HP-5 MS, 30 m × 0.25 mm × 0.25 μm, Agilent, USA).

Concentration of chloride ion was analyzed with an ion chromatograph (IC, HIC-VP Super Shimadzu, Japan) equipped with a Shim-Pack IC-A3 non-suppressor column (4.6 mm × 150 mm) and a CDD-10A*VP* conductivity detector.

3. Results and discussion

3.1. The characterization of the MWCNTs/graphite and Pd/MWCNTs/graphite

The SEM and TEM images of MWCNTs are presented in Fig. 1. Fig. 1a shows that MWCNTs without purification are stacked onto each other, accompanied by carbon nanoparticles and catalyst (Fe) impurities. After purification and oxidation by HNO_3–H_2SO_4, the clean MWCNTs morphologys are observed in Fig. 1b and c. HR-TEM image of MWCNTs exhibits good crystalline phase and no amorphous carbon is observed (Fig. 1c). EDX analysis reveals that no iron element is detected. This MWCNTs structure after purification is beneficial to improving aspect ratio of the resultant electrocatalytic catalyst. The diameter of MWCNTs is about 40–60 nm. In order to investigate the change of surface chemical properties of MWCNTs, the FT-IR spectra were measured before and after the modification (Fig. 2). The results indicate that purification and oxidation with HNO_3–H_2SO_4 can produce some functional groups on the surface of the MWCNTs material (Fig. 2b). In comparison with the MWCNTs without purification (Fig. 2a), the MWCNTs after purification and oxidation show clearly the presence of a new peak at 1380–1390 cm^{-1} corresponding to the $–OSO_3H$ group besides the carbonyl and carboxyl groups at 1600–1700 cm^{-1} and the hydroxyl and phenolic bands at 3300–3600 cm^{-1}. Such surface functionalization can enhance the reactivity, improve the specificity and provide an approach for further chemical

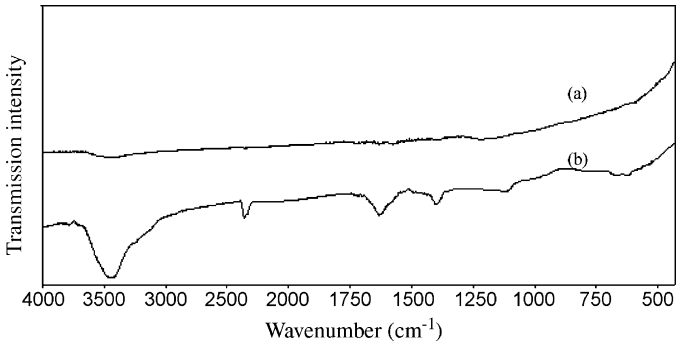

Fig. 2. FT-IR spectra of MWCNTs (a) without purification and (b) after purification and oxidation with HNO_3–H_2SO_4.

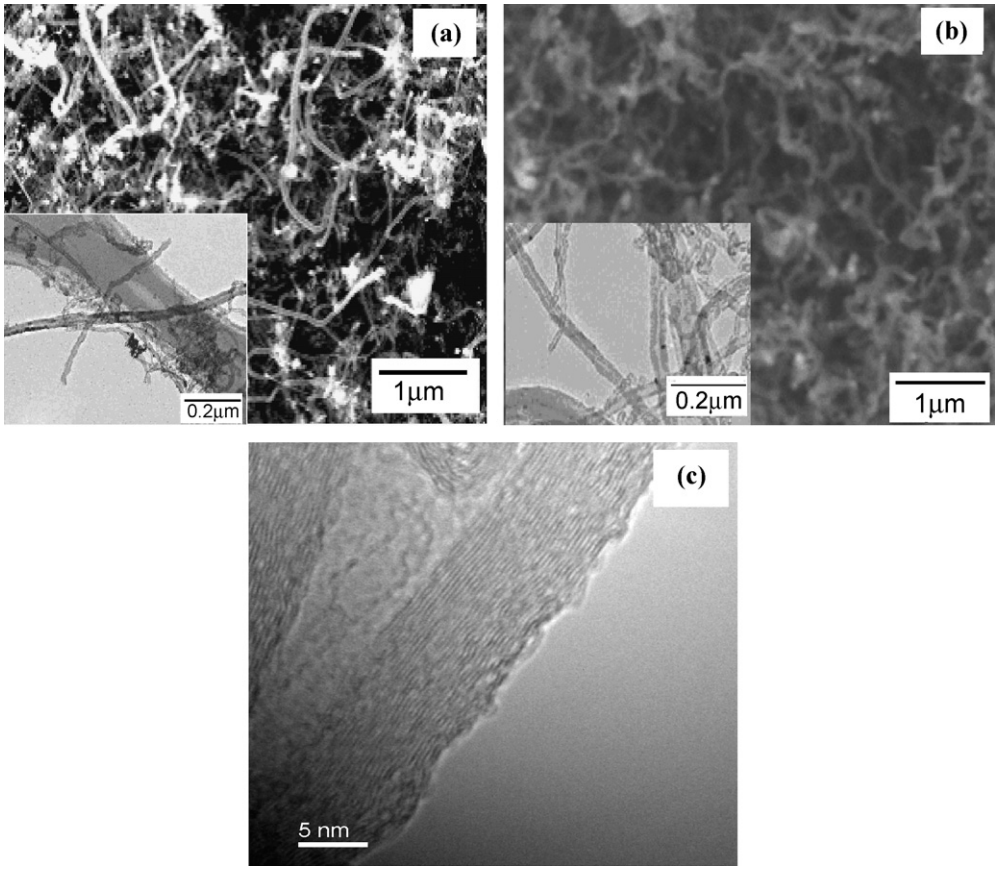

Fig. 1. SEM and TEM images of MWCNTs (a) without purification, (b) after purification/oxidation and (c) an image High-resolution (HR) TEM after purification/oxidation.

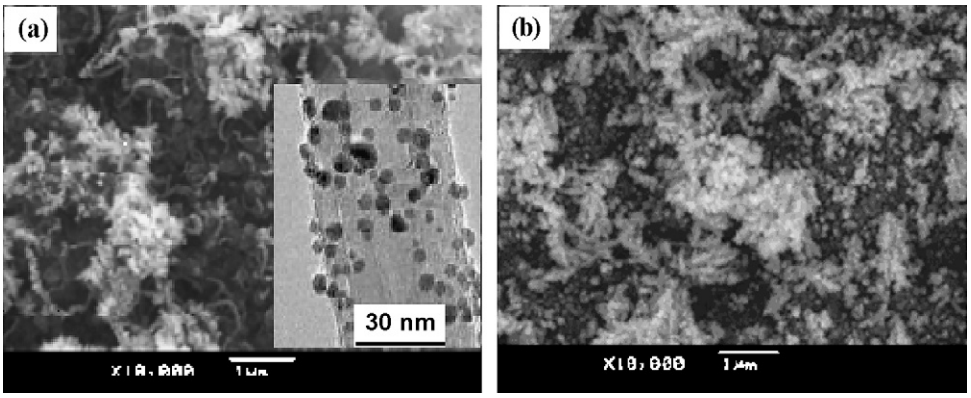

Fig. 3. SEM and TEM images of (a) Pd/MWCNTs/graphite and (b) Pd/graphite.

modification of the carbon nanotubes, such as ion adsorption, metal deposition, and hydrophilicity [30]. The BET surface area of purified MWCNTs is 45 m^2/g and increased by 20% (54 m^2/g) after surface oxidation with HNO_3–H_2SO_4.

Fig. 3 shows the SEM images of the Pd/MWCNTs/graphite and Pd/graphite electrode with the same Pd amount (2 mg/cm^2). The results show that Pd particles are well dispersed on the surface of MWCNTs and graphite. Fig. 3a shows the TEM image that Pd disperses uniformly on the surface of MWCNTs.

The XRD patterns of Pd/MWCNTs/graphite and Pd/graphite are shown in Fig. 4. All the patterns show clearly typical peaks of (0 0 2), (1 0 0), (1 0 1) and (1 1 0) phase of MWCNTs or graphite [31]. The peaks at 39.8°, 46.2°, 68.1° and 82.02° can be attributed to (1 1 1), (2 2 0), (2 0 0) and (3 1 1) phase of Pd, respectively [32]. The average crystallite size of the Pd particles on Pd/MWCNTs/graphite and Pd/graphite was calculated by the Scherrer formula [33]. The results suggest that the particle size of Pd (about 50 nm) on graphite electrode is larger than that on MWCNTs (about 13 nm). This small particle size of Pd on MWCNTs is known to be highly active for the hydrogenation reactions [34].

3.2. HDH of PCP at Pd/graphite and Pd/MWCNTs/graphite electrode

Under a constant potential of −0.8 V, the HDH of PCP was carried out at Pd/graphite and Pd/MWCNTs/graphite electrode with the same Pd amount (2 mg/cm^2), respectively. As shown in Fig. 5, within 180 min, PCP is completely degraded and dechlorination efficiency reaches 96% (current efficiency is up to 7.4%) at the Pd/MWCNTs/graphite electrode. In contrast, only 81% PCP is degraded and dechlorination efficiency is only 68% at the Pd/graphite. Moreover, the yield of intermediates including chlorophenols, phenol, and cyclohexanone at the Pd/graphite electrode are 11%, 59%, and 30% against 3%, 37% and 60% at the Pd/MWCNTs/graphite electrode, respectively. As can be seen from the above results, the product yield of cyclohexanone at Pd/MWCNTs/graphite electrode is 2 times of that at Pd/graphite electrode. The homogeneous distribution of Pd nanoparticles, the unique structure of carbon nanotubes and the three-dimensional nanostructure of the Pd/MWCNTs/graphite electrode may be contribute to the high dechlorination efficiency and further hydrogenation hydrogenation activity of the carbon–carbon double bond for PCP [27,28].

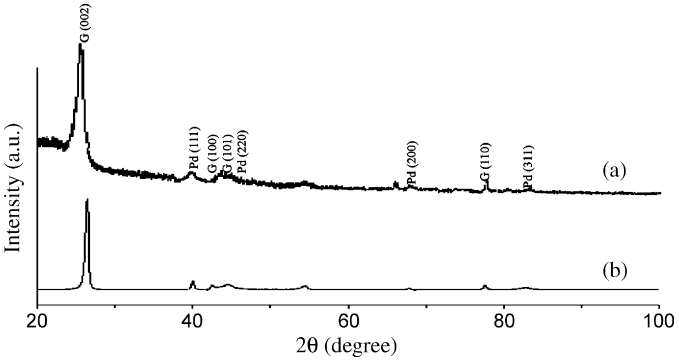

Fig. 4. XRD patterns of (a) Pd/MWCNTs/graphite and (b) Pd/graphite.

3.3. Influence of anolyte

It has been found that during the HDH of PCP, the pH of catholyte greatly depended on anolyte. Fig. 6 shows the pH increases rapidly due to the hydrogen evolution when the

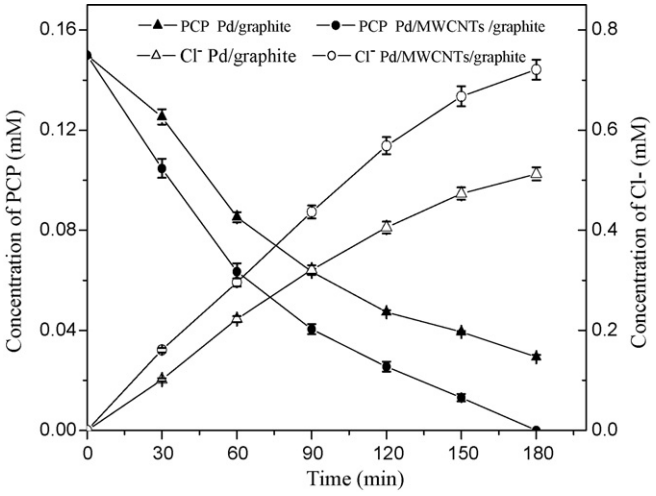

Fig. 5. HDH of PCP at Pd/graphite and Pd/MWCNTs/graphite electrodes. (anolyte 0.2 M H_2SO_4; C_0 = 0.15 mM; catholyte 0.05 M Na_2SO_4 (pH 3); catholyte volume 50 mL; Pd 2 mg/cm^2; constant potential −0.8 V vs. SCE).

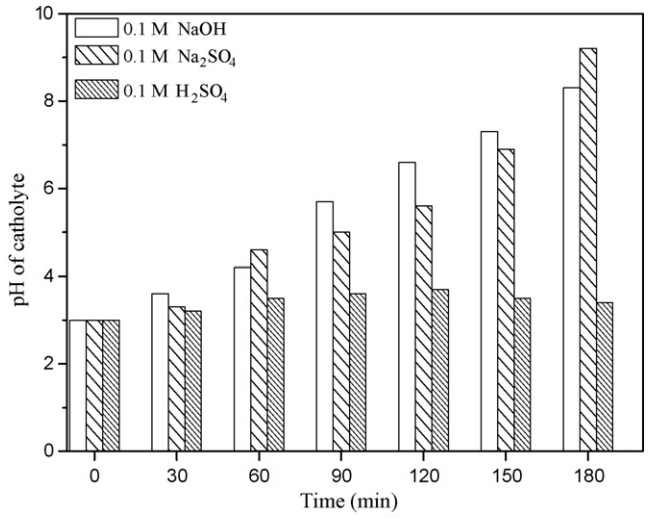

Fig. 6. pH variation of catholyte during the HDH of PCP at Pd/MWCNTs/graphite electrode with different anolytes. (catholyte 0.05 M Na_2SO_4 (pH 3); constant potential −0.8 V vs. SCE).

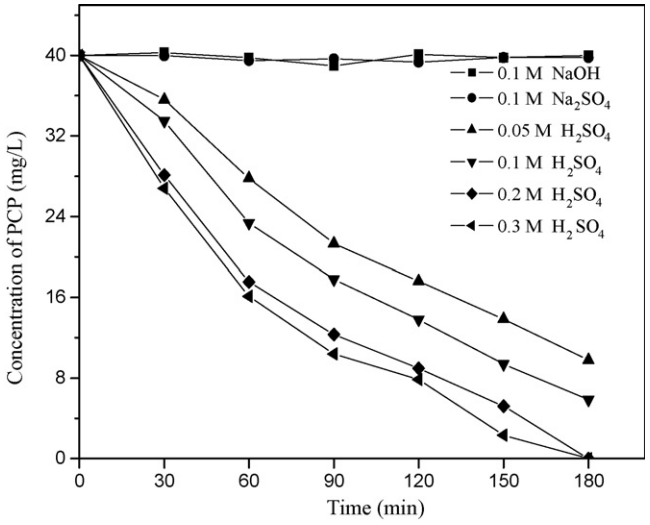

Fig. 7. Effect of anolyte on the HDH of PCP at Pd/MWCNTs/graphite electrode. (catholyte 0.05 M Na_2SO_4 (pH 3); constant potential −0.8 V vs. SCE).

anolyte is neutral or basic. However, in the acidic anolyte, the pH changes slightly because the anolyte H^+ ions cross the Nafion membrane into the catholyte, which might partly counteract the effect of the hydrogen evolution.

To observe the effects of anolyte on the HDH of PCP, the experiments were conducted with the same initial PCP concentration in different anolytes. As shown in Fig. 7, PCP is hardly degraded in the anolyte of Na_2SO_4 or NaOH. However, the HDH of PCP is evident when the anolyte is H_2SO_4. Moreover, the degradation efficiency of PCP increases as the concentration of H_2SO_4 rises from 0.05 to 0.2 M. When the concentration of H_2SO_4 is higher than 0.2 M, the concentration of H_2SO_4 has no obvious effect on degradation efficiency of PCP. From the view of the ECH mechanism (Eqs. (1–3)), active hydrogen plays a very important role during the HDH of PCP. The active hydrogen formation was depended on pH value, namely lower pH value could accelerate the electroreduction of hydrogen ions, and finally the plentiful produced hydrogen (or hydrogen atoms) would be propitious to hydrogenation reaction. When the potential is lower than −0.8 V in neutral or basic solution, H_2O could not be electrolyzed to create enough active hydrogen. Therefore, the HDH of PCP is not evolutive in the neutral or basic electrolyte. However, when the anolyte is acid, the active hydrogen, which is evolved from the H^+ in the cathodic room migrated through the Nafion membrane, can effectively degrade PCP.

3.4. Influence of cathode potential

The HDH of PCP at different cathode potential is presented in Fig. 8. As shown in Fig. 8a, the higher potential causes higher HDH of PCP as the potential rises from −0.2 to −0.8 V, but further increase of potential to −1.0 V reduces HDH of PCP. This may be due to that the amount of activated hydrogen increases with the potential increasing, which benefits to the reactions of Eqs. (1–3). However, when the bias potential is higher than −0.8 V, the secondary reactions (Eqs. (5 and 6)) are accelerated during the HDH of PCP, which decreases the degradation efficiency of PCP. Similar results have been reported in the electrocatalytic HDH of DCP at Ti/Pd electrode [35]. The influence of the cathode potential on the product distributions of the HDH process is shown in Fig. 8b, it can been seen, that higher potential causes higher HDH of PCP to phenol, and that the phenol is further hydrogenated to cyclohexanone.

3.5. Stability of electrode

To evaluate the stability of electrode, the HDH of PCP was repeated 6 times with the Pd/MWCNTs/graphite and Pd/graphite electrode. After each run of 180 min, the liquid phase was removed and the electrode was thoroughly rinsed successively with 1 M NaOH, ethanol and water. Both electrodes exhibited a decline in activity with reuse. The conversion of PCP decreased from 100% to 73% and dechlorination efficiency decreased from 96% to 60% when the Pd/MWCNTs/graphite was used 6 times. In contrast, the conversion of PCP decreased from 81% to 52% at the Pd/graphite and dechlorination efficiency decreased from 68% to 37%. The results of AAS analysis show that 8.5% of the initial amount of Pd leaches from MWCNTs, and 14.6% leacheds from graphite, respectively. It can be seen that the Pd/MWCNTs/graphite electrode exhibited higher stability than Pd/graphite. It has been reported that Pd/C suffered a 20% Pd loss during a 20 h HDC of polychlorinated biphenyls (PCB) [36] and 12% loss of Pd from Pd/C in liquid phase HDH of dichlorophenol [37]. The Pd/MWCNTs/graphite electrode after being used 6 times was observed using SEM no obvious damage or change in the structure and morphology. The high-resolution TEM image (Fig. 9) shows MWCNTs with a higher degree of graphitization. Moreover, the image indicates that the

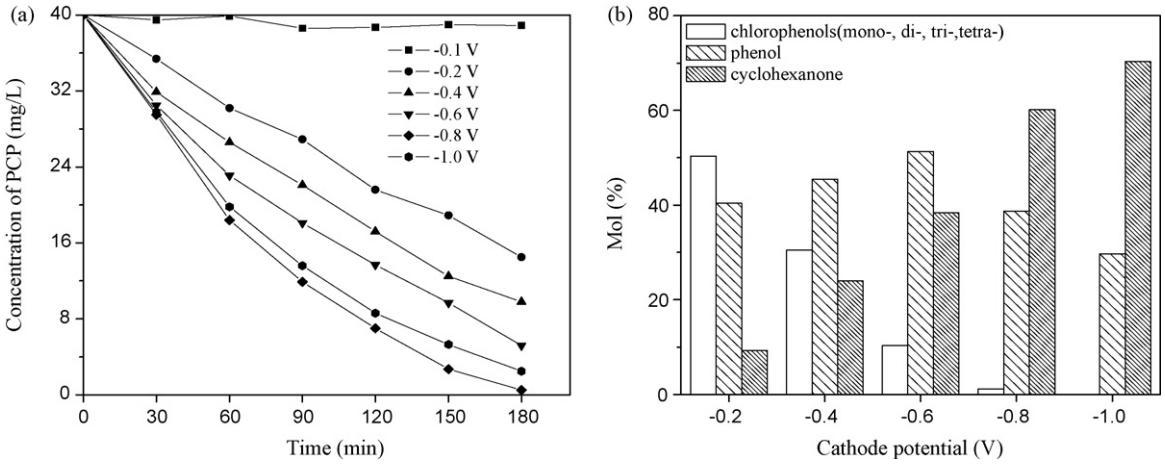

Fig. 8. Effect of cathode potential on (a) the HDH of PCP and (b) the product distribution at Pd/MWCNTs/graphite electrode. (anolyte 0.2 M H_2SO_4; catholyte 0.05 M Na_2SO_4 (pH 3)).

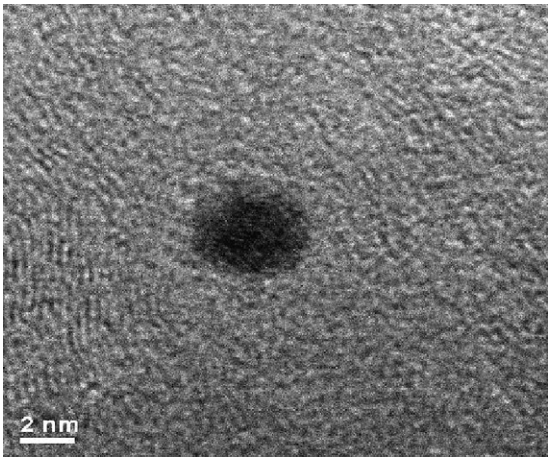

Fig. 9. HR-TEM images of Pd/MWCNTs.

Pd particles are a strong metal-support interaction with the wall surface of the carbon nanotubes. Such MWCNTs with nanoscale Pd plays an important role in the improvement of HDH of PCP. The above results reveal that the Pd/MWCNTs/graphite electrode is acceptable stable after being repeated experiments, which may be due to high degree of graphitization of MWCNTs and compact interaction of Pd particles and carbon nanotubes.

3.6. Identification of intermediate products by GC/MS

The extracts from the electrolyte solution were analyzed by GC/MS and identified by a good quality match (>90%) from NIST 98 mass spectra library. After 90 min of electrolysis, five main hydrogenation products were detected including tetrachlorophenols, trichlorophenols, dichlorophenols, phenol and cyclohexanone. After 180 min, cyclohexanone, phenol and small amount of trichlorophenols were detected. On the basis of the above results, the PCP was gradually degraded to PNL, and further hydrogenation of the carbon–carbon double bond to cyclohexanone.

4. Summary

The MWCNTs electrode was prepared directly by chemical vapor deposition on graphite. The palladized MWCNTs electrode was investigated for electrocatalytic HDH of PCP. The MWCNTs exhibit excellent properties, including small particle size and good dispersion of deposited Pd and three-dimensional electrode structure, which is benefit to electrocatalytic HDH of PCP. Therefore, Pd/MWCNTs/graphite electrode exhibited better catalytic activity for electrocatalytic HDH of PCP than Pd/graphite electrode. PCP at low concentration in aqueous solution can be completely dechlorinated and even further hydrogenated rapidly to more lower toxic and valuable cyclohexanone under mild conditions. Hence, the carbon nanotubes may be acceptable candidates for electrocatalyst supports that possess high electrocatalytic activity, high surface area and acceptable chemical stability. This process shows an applicable potential for the purification of industrial effluents containing high toxic organic pollutants with halogen.

Acknowledgments

This work was financially supported by Nature Science Foundation of China (No. 20337020 and No. 20525723) and National Basic Research Program of China (2003CB415006).

References

[1] J. Morales, R. Hutcheson, I.F. Cheng, J. Hazard. Mater. 90 (2002) 97.
[2] D.J. Crosby, K.L. Beynon, P.A. Greve, F. Korte, G.G. Stili, J.W. Vouk, Pure Appl. Chem. 53 (1981) 1051.
[3] T. Kishino, K. Kobayshi, Water Res. 30 (1996) 393.
[4] L.N. Zanaveskin, V.A. Averganov, Y.A. Treger, Russ. Chem. Rev. 65 (1996) 17.
[5] K. Mackenzie, H. Frenzel, F.D. Kopinke, J. Appl. Catal. B Environ. 63 (2006) 161.
[6] V. Felis, C.D. Bellefon, P. Fouilloux, D. Schweich, J. Appl. Catal. B Environ. 20 (1999) 91.
[7] H. Yu, E.M. Kennedy, M.A. Uddin, B.Z. Dlugogorski, J. Appl. Catal. B Environ. 44 (2003) 253.

[8] M.A. Keane, Appl. Catal. A Gen. 271 (2004) 109.
[9] H.M. Roy, C.M. Wai, T. Yuan, J.K. Kim, W.D. Marshall, Appl. Catal. A Gen. 271 (2004) 137.
[10] F.J. Urbano, J.M. Marinas, J. Mol. Catal. A Chem. 173 (2001) 329.
[11] E.J. Shin, A. Spiller, G. Tavoularis, M.A. Keane, Phys. Chem. Chem. Phys. 1 (1999) 3173.
[12] I.F. Cheng, Q. Fernando, N. Korte, Environ. Sci. Technol. 31 (1997) 1074.
[13] A.I. Tsyganok, K. Otsuka, J. Appl. Catal. B Environ. 22 (1999) 15.
[14] R. Chetty, P.A. Christensen, B.T. Golding, K. Scott, Appl. Catal. A: Gen. 271 (2004) 185.
[15] P. Dabo, A. Cyr, F. Laplante, F. Jean, E.H. Menard, J. Lessard, Environ. Sci. Technol. 34 (2000) 1265.
[16] G. Chen, Z.Y. Wang, D.G. Xia, Electrochim. Acta 50 (2004) 933.
[17] B. Mahdavi, P. Chambrion, J. Binette, E. Martel, J. Lessard, Can. J. Chem. 73 (1995) 846.
[18] S. Iijima, Nature 354 (1991) 56.
[19] H. Dai, J.H. Hafner, A.G. Rinzler, D.T. Colbert, R.E. Smalley, Nature 384 (1996) 147.
[20] A. Fonseca, K. Hernadi, J.B. Nagy, D. Bernaerts, A.A. Lucas, J. Mol. Catal. A Chem. 107 (1996) 159.
[21] A. Chambers, C. Park, R.T.K. Baker, N.M. Rodriguez, J. Phys. Chem. B 122 (1998) 4253.
[22] B. Revathi, L. Christophe, M. Ryuta, S. Hiroshi, L.L. Mikako, J. Phys. Chem. B 108 (2004) 12718.
[23] M. Motta, Y.L. Li, L. Kinloch, A. Windle, J. Am. Chem. Soc. 5 (2005) 1529.
[24] H.F. Cui, J.S. Ye, W.D. Zhang, J. Wang, F.S. Sheu, J. Electroanol. Chem. 577 (2005) 295.
[25] G.L. Che, B.B. Lakshmi, C.R. Martin, E.R. Fisher, Langmuir 15 (1999) 750.
[26] A.M. Zhang, J.L. Dong, Q.H. Xua, H.K. Rhee, X.L. Li, Catal. Today 93–95 (2004) 347.
[27] C.H. Li, Z.X. Yu, K.F. Yao, S.F. Ji, J. Liang, J. Mol. Catal. A Chem. 226 (2005) 101.
[28] C. Amorim, G. Yuan, P.M. Patterson, M.A. Keane, J. Catal. 234 (2005) 268.
[29] R. Andrews, D. Jacques, A.M. Rao, F. Derbyshire, D. Qian, X. Fan, E.C. Dickey, J. Chen. Chem. Phys. Lett. 303 (1999) 467.
[30] T.W. Ebbesen, P.M. Ajayan, Nature 358 (1992) 220.
[31] W.K. Hsu, W.Z. Li, Y.Q. Zhu, N. Grobert, M. Terrones, H. Terrones, N. Yao, J.P. Zhang, S. Firth, R.J.H. Clark, A.K. Cheetham, J.P. Hare, H.W. Kroto, D.R.M. Walton, Chem. Phys. Lett. 317 (2000) 77.
[32] T. Arunagiri, T.D. Golden, O. Chyan, Mater. Chem. Phys. 92 (2005) 152.
[33] B.D. Cullity, Elements of X-ray Diffraction, second ed., Addison-Wesley, London, 1978.
[34] D.J. Guo, H.L. Li, J. Colloid Interf. Sci. 286 (2005) 274.
[35] H. Cheng, K. Scyott, P.A. Christensen, J. Electrochem. Soc. 150 (2003) 25.
[36] P. Forni, L. Prati, M. Rossi, Appl. Catal. B Environ. 14 (1997) 49.
[37] G. Yuan, M.A. Keane, Catal. Today 88 (2003) 27.